Computer Assisted Mechanics and Engineering Sciences, 13: 379–394, 2006.

Boundary element formulation for dynamic analysis of inelastic structures

Tomasz Czyż, Piotr Fedeliński
Department for Strength of Materials and Computational Mechanics
Silesian University of Technology
ul. Konarskiego 18A, 44-100 Gliwice, Poland

(Received March 17, 2006)

The boundary element formulation for dynamic analysis of inelastic two-dimensional structures subjected to stationary or transient inertial loads is presented. The problem is solved by using simultaneously the displacement and stress integral equations. The numerical solution requires discretization of the boundary displacements and tractions, and stresses in the interior of the body. The boundary is divided into quadratic elements and the domain into constant or quadratic quadrilateral cells. The unknown stresses in the coupled system of equations are computed using an iterative procedure. The mass matrix of the structure is formulated by using the dual reciprocity method. The matrix equation of motion is solved step-by-step by using the Houbolt direct integration method. Several numerical examples show the influence of the discretization on the accuracy and new applications of the method. The solutions are compared to the analytical results or those computed by the finite element method.

Keywords: boundary element method (BEM), dual reciprocity method (DRM), inelasticity, elastoplasticity, dynamic analysis

1. Introduction

The dynamic analysis of elastoplastic structures is a significant subject of engineering research in recent decades. To obtain more reliable results of computer aided analysis of structures under transient dynamic loadings one must take into account nonlinearities due to inelasticity of the material. The finite element method (FEM) is the most popular numerical method for the solution of elastoplastic dynamic problems, but recently the boundary element method (BEM) becomes also a very suitable method to solve this class of problems. Main advantages of this method are accuracy of stress analysis and small number of degrees of freedom of the numerical model.

The fundamentals the BEM formulation for nonlinear materials are presented in the textbooks by Telles [23], Banerjee [2] and Gao and Davies [12]. The most popular approaches in the elastoplastic BEM are the initial stress and initial strain formulation, because of easy physical interpretation and simple implementation. Each approach requires the plastic domain discretization, but this procedure does not increase the number of degrees of freedom. The integral equations are formulated in the incremental form and the numerical solution is obtained by the iterative methods.

Dynamic solution of the elastoplastic problem can be obtained by the BEM by using different techniques. An overview of formulations and applications of the BEM to inelastic problems was presented by Beskos [3, 4]. In the first method, presented by Ahmad and Banerjee [1], Telles, Carrer and Mansur [26] and Israil and Banerjee [16], the fundamental solutions of elastodynamics are used. This approach, called the time domain boundary element method (TD-BEM), eliminates the inertial domain integral and allows analysis of infinite or semi-infinite domains. However, the computational cost is very high due to complex kernels involved. The second class of techniques uses the elastostatic fundamental solutions. Simplicity of these solutions leads to computational advantages, although the inertial domain integral is created. The inertial domain integral can be computed

by the domain discretization by using cells and is called the domain boundary element method (D-BEM). This approach was used by Carrer, Telles [6, 24, 25], Coda and Venturini [7] and Hatzigeorgiou and Beskos [15]. The inertial domain integral can be transformed into boundary integrals by approximating the accelerations within the domain, which is the basis of the dual reciprocity boundary element method (DR-BEM). This method was proposed by Kontoni and Beskos [17–21] for the elastoplastic analysis. In comparison to the D-BEM the number of unknowns in the resultant algebraic system depends only on the boundary discretization and interior cells are required only in the plastic domain.

This work presents the application of the DR-BEM to two-dimensional dynamic elastoplasticity. The paper shows the integration of domain integrals in the plastic region in detail and the influence of its discretization on the solutions. Preliminary results of this research were presented by Czyż and Fedeliński in [8–10]. New examples of application of the DR-BEM are given in this work.

2. Governing equations

Consider an elastoplastic, isotropic and homogeneous body with the boundary Γ occupying the domain Ω which is subjected to body forces or dynamic tractions, shown in Fig. 1. The theory of small displacements is assumed.

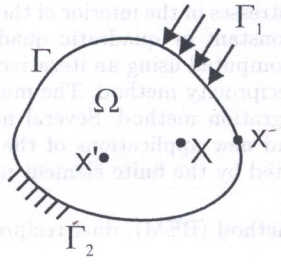

Fig. 1. Elastoplastic body

The following boundary conditions,

$$\begin{aligned} t_i(x,\tau) = \sigma_{ij}(x,\tau)\, n_j = \bar{t}_i(x,\tau) \qquad & \text{on } \Gamma_1\,, \\ u_i(x,\tau) = \bar{u}_i(x,\tau) \qquad & \text{on } \Gamma_2\,, \end{aligned} \tag{1}$$

and initial conditions

$$u_i(x,0) = u_i^0(x) \quad \text{and} \quad \dot{u}_i(x,0) = v_i^0(x) \qquad \text{in } \Omega, \tag{2}$$

are imposed, where u_i is the component of displacement, t_i is the component of traction, $\bar{u}_i$ and $\bar{t}_i$ denote the prescribed boundary conditions, σ_{ij} is the stress tensor, n_i is the component of the outward normal versor at the boundary, Γ_1 and Γ_2 are parts of the boundary Γ ($\Gamma_1 \cup \Gamma_2 = \Gamma$), u_i^0 and v_i^0 are prescribed initial conditions, x are coordinates of a point, τ is time, repeated indices denote the summation convention and overdots – time derivatives.

The equation of motion of the body has the form

$$\sigma_{ij,j} + b_i = \rho \ddot{u}_i\,, \tag{3}$$

where ρ is a mass density, b_i is the component of body force and an index proceeded by a comma denotes differentiation with respect to the appropriate coordinate.

The constitutive equations are based on the incremental stress-strain relations for inviscid plasticity and elastoplastic flow theory [23]

$$\mathrm{d}\sigma_{ij} = C_{ijkl}^{\mathrm{ep}}\, \mathrm{d}\varepsilon_{kl}\,, \tag{4}$$

where $\mathrm{d}\varepsilon_{kl}$ is the total strain increment.

For the isotropic hardening

$$C^{\mathrm{ep}}_{ijkl} = C_{ijkl} - \frac{1}{\gamma'} C_{ijmn} a_{mn} a_{op} C_{opkl}\,, \tag{5}$$

where C_{ijkl} is the elastic tensor,

$$C_{ijkl} = \frac{2G\nu}{1-2\nu}\,\delta_{ij}\delta_{kl} + G\left(\delta_{ik}\delta_{jl} + \delta_{il}\delta_{jk}\right), \tag{6}$$

G is the Kirchhoff shear modulus of elasticity, ν is the Poisson ratio, δ_{ij} is the Kronecker delta and a_{mn} is a derivative of the yield function F with respect to the appropriate component of the stress tensor,

$$a_{mn} = \frac{\partial F}{\partial \sigma_{mn}}\,. \tag{7}$$

The parameter γ' also depends on derivatives of the yield function, the elastic tensor and the hardening slope H

$$\gamma' = a_{ij} C_{ijkl} a_{kl} + H. \tag{8}$$

Introducing the elastic stress increment,

$$\mathrm{d}\sigma^{\mathrm{e}}_{ij} = C_{ijkl}\,\mathrm{d}\varepsilon_{kl}\,, \tag{9}$$

the plastic stress increment can be calculated as

$$\mathrm{d}\sigma^{\mathrm{p}}_{ij} = \mathrm{d}\sigma^{\mathrm{e}}_{ij} - \mathrm{d}\sigma_{ij} = \frac{1}{\gamma'} C_{ijmn} a_{mn} a_{kl}\,\mathrm{d}\sigma^{\mathrm{e}}_{kl}\,. \tag{10}$$

3. Boundary integral equations

The relation between the mechanical fields can be obtained using the displacement integral equation. For the initial stress approach and zero initial conditions, the equation has the form [20],

$$\begin{aligned} c_{ij}(x')\,u_j(x',\tau) = {} & \int_\Gamma U_{ij}(x',x)\,t_j(x,\tau)\,\mathrm{d}\Gamma(x) - \int_\Gamma T_{ij}(x',x)\,u_j(x,\tau)\,\mathrm{d}\Gamma(x) \\ & + \rho\int_\Omega U_{ij}(x',X)\,b_j(X)\,\mathrm{d}\Omega(X) - \rho\int_\Omega U_{ij}(x',X)\,\ddot{u}_j(X,\tau)\,\mathrm{d}\Omega(X) \\ & + \int_\Omega E_{jki}(x',X)\,\sigma^{\mathrm{p}}_{jk}(X,\tau)\,\mathrm{d}\Omega(X), \end{aligned} \tag{11}$$

where c_{ij} is a constant, which depends on the position of the collocation point, U_{ij}, T_{ij}, E_{jki} are fundamental solutions of elastostatics, x' is the collocation point, x is a boundary point and X is a domain point (Fig. 1). Since the fundamental solutions U_{ij} and T_{ij} are well known (see for example [12]) only E_{jki} for plane strain is given [23],

$$E_{jki} = -\frac{1}{8\pi(1-\nu)Gr}\left[(1-2\nu)(r_{,k}\delta_{ij} + r_{,j}\delta_{ik}) - r_{,i}\delta_{jk} + 2r_{,i}r_{,j}r_{,k}\right], \tag{12}$$

where r is the distance between the points x' and X. The fundamental solution for plane stress is obtained by replacing ν by $\bar{\nu} = \nu/(1+\nu)$.

Contrary to the elastodynamic case, Eq. (11) contains the domain plastic term, which depends on the unknown plastic stress σ^{p}_{jk}. In order to obtain the stress fields in the domain the stress integral equation is used. For the initial stress approach the equation is [20]

$$\sigma_{ij}(x',\tau) = \int_\Gamma U_{ijk}(x',x)\, t_k(x,\tau)\, \mathrm{d}\Gamma(x) - \int_\Gamma T_{ijk}(x',x)\, u_k(x,\tau)\, \mathrm{d}\Gamma(x)$$
$$+ \rho \int_\Omega U_{ijk}(x',X)\, b_k(X)\, \mathrm{d}\Omega(X) - \rho \int_\Omega U_{ijk}(x',X)\, \ddot{u}_k(X,\tau)\, \mathrm{d}\Omega(X)$$
$$+ \int_\Omega E_{ijkl}(x',X)\, \sigma^{\mathrm{p}}_{kl}(X,\tau)\, \mathrm{d}\Omega(X) + F_{ijkl}\, \sigma^{\mathrm{p}}_{kl}(x',\tau) \tag{13}$$

where U_{ijk}, T_{ijk}, E_{ijkl} and F_{ijkl} are other fundamental solutions. Since the fundamental solutions U_{ijk}, and T_{ijk} are well known (see for example [12]) only E_{ijkl} and F_{ijkl} for plane strain are given here [12],

$$E_{ijkl} = \frac{1}{4\pi(1-\nu)r^2}\left[(1-2\nu)(\delta_{ik}\delta_{lj} + \delta_{jk}\delta_{li} - \delta_{ij}\delta_{kl} + 2\delta_{ij}r_{,k}r_{,l})\right.$$
$$\left. + 2\nu(\delta_{li}r_{,j}r_{,k} + \delta_{jk}r_{,l}r_{,i} + \delta_{ik}r_{,l}r_{,j} + \delta_{jl}r_{,i}r_{,k}) + 2\delta_{kl}r_{,i}r_{,j} - 8r_{,i}r_{,j}r_{,k}r_{,l}\right], \tag{14}$$

$$F_{ijkl} = -\frac{1}{8(1-\nu)}\left[(\delta_{ik}\delta_{jl} + \delta_{il}\delta_{jk}) + (1-4\nu)\delta_{ij}\delta_{kl}\right]. \tag{15}$$

The inertial domain integral in Eq. (11) is transformed into boundary integrals using the dual reciprocity method (DRM) proposed by Nardini and Brebbia [5, 22]. In this method the acceleration is approximated by the following function,

$$\ddot{u}_i(x,\tau) = \ddot{\alpha}^n_i(\tau)\, f^n(x^*,x), \tag{16}$$

where $\ddot{\alpha}^n_i$ is a time-dependent function and f^n is a coordinate function. In the present work it is assumed that

$$f^n(x^*,x) = r + C, \tag{17}$$

where r is the distance between a defining point x^* and the point x, and C is a constant. The defining point can be a boundary or a domain point.

After the transformation the inertial domain term in Eq. (11) has the form

$$\rho \int_\Omega U_{ij}(x',X)\, \ddot{u}_j(X,\tau)\, \mathrm{d}\Omega(X) = \rho \left[c_{ij}(x')\, \hat{u}^n_{jl}(x^*,x') - \int_\Gamma U_{ij}(x',x)\, \hat{t}^n_{jl}(x^*,x)\, \mathrm{d}\Gamma(x)\right.$$
$$\left. + \int_\Gamma T_{ij}(x',x)\, \hat{u}^n_{jl}(x^*,x)\, \mathrm{d}\Gamma(x)\right] \ddot{\alpha}^n_l(\tau), \tag{18}$$

where: $\hat{u}^n_{jl}$ and $\hat{t}^n_{jl}$ are fictitious displacements and tractions [11], respectively, corresponding to the fictitious body force defined by Eq. (17). Similarly the inertial domain term in Eq. (13) can be transformed into the boundary integral form

$$\rho \int_\Omega U_{ijk}(x',X)\, \ddot{u}_k(X,\tau)\, \mathrm{d}\Omega(X) = \rho \left[\hat{\sigma}^n_{ijl}(x^*,x') - \int_\Gamma U_{ijk}(x',x)\, \hat{t}^n_{kl}(x^*,x)\, \mathrm{d}\Gamma(x)\right.$$
$$\left. + \int_\Gamma T_{ijk}(x',x)\, \hat{u}^n_{kl}(x^*,x)\, \mathrm{d}\Gamma(x)\right] \ddot{\alpha}^n_l(\tau), \tag{19}$$

where $\hat{\sigma}^n_{ijl}$ is a fictitious stress.

4. Numerical implementation

In order to obtain the numerical solution, the boundary is divided into 3-node boundary elements and the part of the body where the inelastic behavior is expected is discretized into 1-node or 8-node quadrilateral cells, as shown in Fig. 2. The domain discretization is consistent with the boundary discretization i.e. two constant cells adjoin one quadratic boundary element (Fig. 2a) and one quadratic cell adjoins one quadratic boundary element (Fig. 2b). The method requires discretization of this part of the domain Ω_p, which is in the plastic state. The boundary coordinates, real and fictitious displacements and tractions are interpolated by using quadratic shape functions and the stresses in the domain using constant or quadratic shape functions.

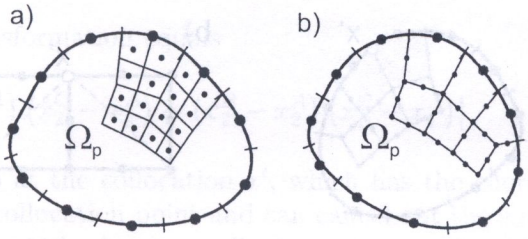

Fig. 2. Discretization of the body; a) constant cells, b) quadratic cells

The displacement integral equation (11) is applied to every boundary node. The resulting system of equations can be written in the matrix form as

$$\mathbf{Hu} + \mathbf{M\ddot{u}} = \mathbf{Gt} + \mathbf{Mb} + \mathbf{E}\sigma^{\mathrm{p}}, \tag{20}$$

where

$$\mathbf{M} = \rho(\mathbf{H\hat{u}} - \mathbf{G\hat{t}})\mathbf{F}^{-1}, \tag{21}$$

$\mathbf{H}$ and $\mathbf{G}$ depend on boundary integrals of the fundamental solutions T_{ij} and U_{ij}, respectively, and boundary shape functions, $\mathbf{M}$ is the mass matrix, $\mathbf{E}$ is dependent on the fundamental solution E_{jki} and domain shape functions, $\mathbf{F}$ contains values of functions f^k at nodes, $\mathbf{u}$ and $\hat{\mathbf{u}}$ contain nodal values of real and fictitious components of displacements, $\mathbf{t}$ and $\hat{\mathbf{t}}$ – nodal values of real and fictitious tractions, $\mathbf{b}$ – nodal values of components of body forces and σ^{p} – components of plastic stress tensor.

The stress integral equations (13) are used to determine stresses at all internal nodes of cells. These equations can be written in the matrix form as

$$\boldsymbol{\sigma} = \mathbf{G't} - \mathbf{H'u} - \mathbf{M'\ddot{u}} + \mathbf{M'b} + \mathbf{E'}\sigma^{\mathrm{p}}, \tag{22}$$

where $\boldsymbol{\sigma}$ contains components of the stress tensor at all internal nodes of cells. The matrices $\mathbf{G'}$, $\mathbf{H'}$, $\mathbf{M'}$ and $\mathbf{E'}$ are obtained similarly as matrices in Eq. (20). They depend on appropriate fundamental solutions in Eq. (13). The stresses in nodes of the cells at the boundary are computed using tractions and displacements.

5. Computation of domain integrals

The fundamental solutions of elastostatics in the displacement and stress integral equations are singular. They tend to infinity when the distance between the collocation point $\mathbf{x'}$ and the boundary $\mathbf{x}$ or domain point $\mathbf{X}$ tends to zero. The boundary integration of fundamental solutions U_{ij}, T_{ij}, U_{ijk} and T_{ijk} is well documented in the literature (see for example [12]) and therefore it is not discussed here.

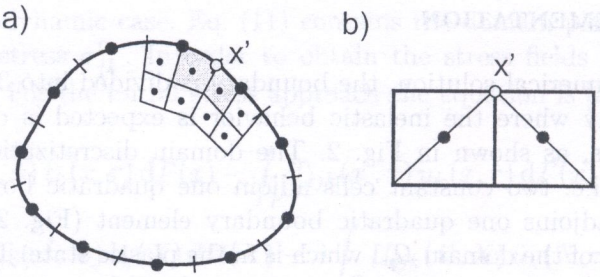

Fig. 3. Boundary collocation point – constant cells; a) singular cells at the collocation point, b) division of cells into triangles

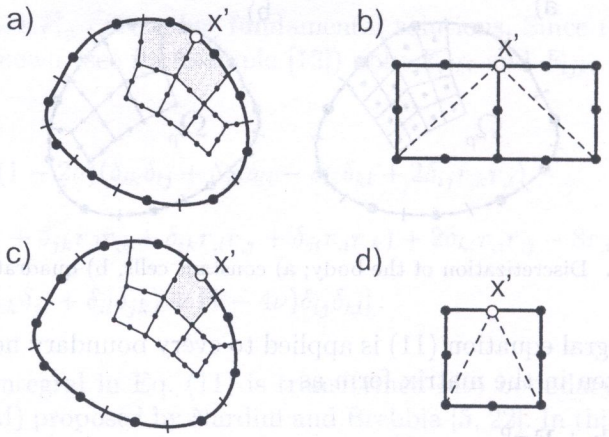

Fig. 4. Boundary collocation point – quadratic cells; a) two singular cells at the collocation point, b) division of two cells into triangles, c) one singular cell at the collocation point, d) division of one cell into triangles

The fundamental solution E_{jki} in the displacement integral equation, defined by Eq. (12), has the order of singularity $O(1/r)$, which is classified as the weak singularity. Special techniques of integration should be used for cells, which are adjacent to collocation points. The following cases should be considered:

for constant cells (Fig. 3):

- the collocation point x' is at the corners of two constant cells (Fig. 3a) – each cell is divided into two triangles (Fig. 3b),

for quadratic cells (Fig. 4):

- the collocation point x' is at the corner of two quadratic cells (Fig. 4a) – each cell is divided into two triangles (Fig. 4b),
- the collocation point is at the mid-side node of the quadratic cell (Fig. 4c) – the adjacent cell is divided into three triangles (Fig. 4d).

The triangles are transformed from the global coordinate system $(x_1\,,\,x_2)$ to the local coordinate system $(\xi_1\,,\,\xi_2)$, as shown in Fig. 5. After the transformation, the triangles become squares [11]. The corner of the triangle C, where the collocation node x' is situated, is transformed into one side of the square $C'C''$. The relationship between the global and local coordinates is expressed as follows,

$$x_i = \frac{1}{4}(1-\xi_1)(1+\xi_2)\,x_i^A + \left[1 - \frac{1}{2}(1+\xi_1) - \frac{1}{4}(1-\xi_1)(1+\xi_2)\right] x_i^B + \frac{1}{2}(1+\xi_1)\,x_i^C\,, \tag{23}$$

where x_i^A, x_i^B and x_i^C are coordinates of the corners A, B, C.

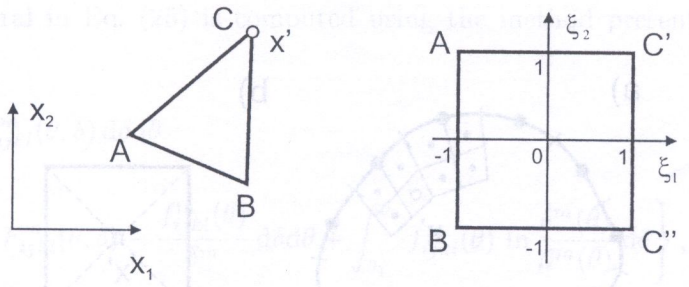

Fig. 5. Transformation of the triangle in the global coordinate system into the square in the local coordinate system

The Jacobian of this transformation equals

$$|J| = \frac{1}{8}(1-\xi_1)\left|\left(x_1^B - x_1^A\right)\left(x_2^C - x_2^A\right) - \left(x_2^B - x_2^A\right)\left(x_1^C - x_1^A\right)\right|, \tag{24}$$

The Jacobian equals zero at the collocation x', which has the coordinate $\xi_1 = 1$. The order of the Jacobian is $O(r)$ at the collocation point and can cancel out the singularity of the fundamental solution E_{jki}. The integrals in the local coordinate system are computed by using the standard Gaussian quadrature.

The fundamental solution E_{ijkl} in the stress integral equation, defined by Eq. (14), has the order of singularity $O(1/r^2)$, which is classified as the strong singularity. Special techniques of integration should be used for cells, which contain or are adjacent to collocation points. The following cases should be considered:

for constant cells (Fig. 6):

- the collocation point x' is at the center of the constant cell (Fig. 6a) – the cell is divided into four triangles (Fig. 6b),

for quadratic cells (Fig. 7):

- the collocation point is at the mid-side node of two quadratic cells (Fig. 7a) – each adjacent cell is divided into three triangles (Fig. 7b),
- the collocation point x' is at the corner of four quadratic cells (Fig. 7c) – each cell is divided into two triangles (Fig. 7d).

The cells are transformed from the global coordinate system (x_1, x_2) to the local coordinate system (ξ_1, ξ_2). Next, the cells are transformed to the polar coordinate system (θ, δ) with the center at the collocation point (ξ_1', ξ_2'). The Jacobian of this additional transformation equals δ. The integral over the domain of cells Ω_s which contain the collocation point is

$$\int_{\Omega_s} E_{ijkl}(x', X)\,\sigma_{kl}^{\mathrm{p}}(X,\tau)\,\mathrm{d}\Omega(X) = \sum_{m=1}^{M}\sum_{n=1}^{N}\int_{\theta_1}^{\theta_2}\int_0^{\hat{\delta}} E_{ijkl}(\xi', \xi)\,N^n(\xi)\,J(\xi)\,\delta\,\mathrm{d}\delta\mathrm{d}\theta\,\sigma_{kl}^{\mathrm{p}n}(\tau), \tag{25}$$

where M is the number of triangular segments at the collocation point, as shown in Figs. 6 and 7, N is the number of nodes in the cell ($N = 1$ for a constant cell and $N = 8$ for a quadratic cell), θ_1 and θ_2 are the angles which define the sides of a triangle, N^n are stress shape functions, J is the Jacobian of the transformation from the coordinate system (x_1, x_2) to (ξ_1, ξ_2), $\sigma_{kl}^{\mathrm{p}n}$ are components of plastic stresses at the nodes of the cell. An arbitrary position of the collocation point in the cell and its division into triangles is shown in Fig. 8. The integrand in Eq. (25) is denoted as

$$F_{ijkl}(\theta, \delta) = E_{ijkl}(\xi', \xi)\,N^n(\xi)\,J(\xi)\,\delta. \tag{26}$$

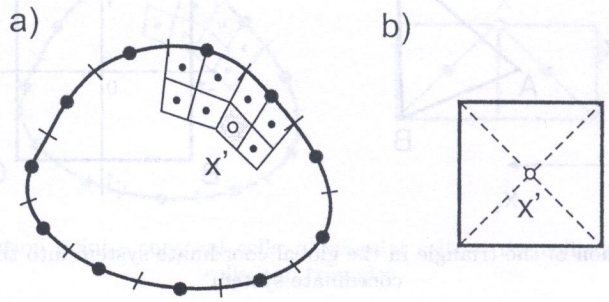

Fig. 6. Internal collocation point – constant cells; a) singular cell at the collocation point, b) division of the cell into triangles

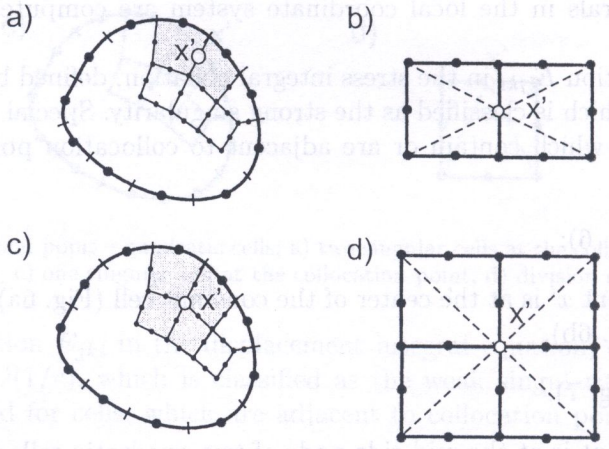

Fig. 7. Internal collocation point – quadratic cells; a) two singular cells at the collocation point, b) division of two cells into triangles, c) four singular cells at the collocation point, d) division of four cells into triangles

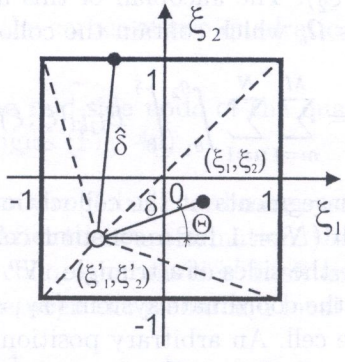

Fig. 8. Polar coordinate system with the origin at the collocation point

The singular integral in Eq. (25) is computed using the method presented by Guiggiani and Gigante [14],

$$I_s = \sum_{m=1}^{M} \int_{\theta_1}^{\theta_2} \int_0^{\hat{\delta}} F_{ijkl}^m(\theta, \delta)\, \mathrm{d}\delta \mathrm{d}\theta$$

$$= \sum_{m=1}^{M} \left\{ \int_{\theta_1}^{\theta_2} \int_0^{\hat{\delta}} F_{ijkl}^m(\theta, \delta) - \frac{f_{ijkl}^m(\theta)}{\delta^m}\, \mathrm{d}\delta \mathrm{d}\theta + \int_{\theta_1}^{\theta_2} f_{ijkl}^m(\theta)\, \ln \frac{\hat{\delta}^m(\theta)}{\beta^m(\theta)}\, \mathrm{d}\delta \right\}, \tag{27}$$

where f_{ijkl}^m is the Taylor expansion of the integrand in the neighbourhood of the collocation point

$$F_{ijkl}^m(\theta, \delta) = \frac{1}{\delta} [f_{ijkl}^m(\theta) + O(\delta)], \tag{28}$$

$\hat{\delta}^m$ is the distance between the collocation point and the boundary of the cell in the local coordinate system and β^m is computed as follows,

$$\beta = \frac{1}{\sqrt{A_1^2(\theta) + A_2^2(\theta)}}, \tag{29}$$

and

$$A_i(\theta) = \frac{\partial x_i}{\partial \xi_1}(\xi_1, \xi_2)\, \cos\theta + \frac{\partial x_i}{\partial \xi_2}(\xi_1, \xi_2)\, \sin\theta. \tag{30}$$

The integrals in Eq. (27) are computed using the Gaussian quadrature.

The accuracy of the solution can be improved by using additional internal collocation points in the displacement integral equation. In this case the division of cells and integration are similar as presented above.

6. Solution procedure

The matrix equation of motion (20) is solved step-by-step by using the direct integration Houbolt method. This method introduces an artificial damping and filters the high mode response of the solution.

In each time-step the unknown displacements, tractions and stresses are computed. The displacement equation and stress equation contains a vector of not known a priori inelastic stresses $\boldsymbol{\sigma}^{\mathrm{P}}$. In order to determine the stresses an iterative procedure is used. The algorithm of the iterative procedure employed in each time-step is shown in Fig. 9.

At the beginning of the iterative procedure the plastic stresses from the previous time step are used. Next the boundary unknowns are computed using Eq. (20) and the elastic stresses using Eq. (22). Later the yield criterion is applied to detect which points are in the plastic state. For each node, where the effective stresses are above the yield stress, the elastic stress increment is computed. The elastic stress increment is the excess of stresses over the stresses, which correspond to the yield stress. Knowing the elastic stress increment, the plastic stress increment can be computed from Eq. (10) and substituted again to Eq. (20) for each node in the plastic state. Next this increment is added to the total plastic stresses in the node. When the plastic stress increment is determined for each node, the boundary unknowns with the new vector of plastic stresses are computed. This procedure is repeated until the change of the results is so small that could be neglected. In the numerical examples only one iteration is applied because further increase of the number of iterations does not influence the accuracy of results.

The present method can be used for structures subjected to static loadings. It this case it is assumed that the loads vary slowly linearly with time. The number of time-step corresponds to consecutive increments of the applied load. If these steps are sufficiently small there is no need to use the iterations. When the increments of load are greater or if only one increment is used, the iterations are necessary to obtain accurate results.

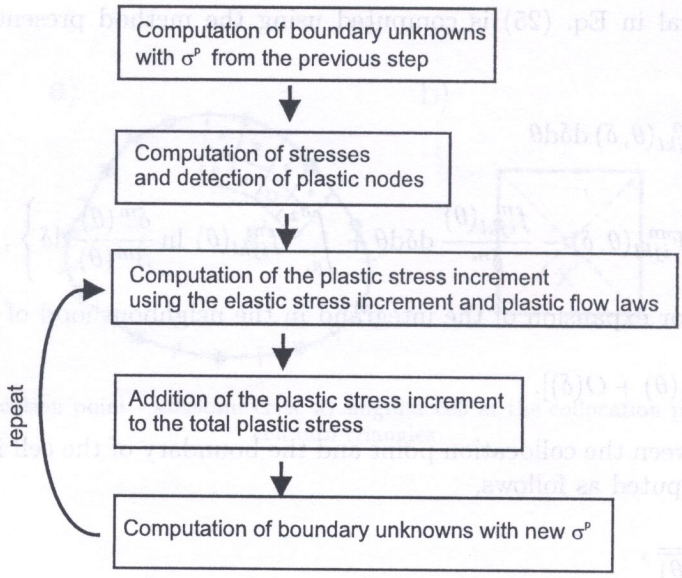

Fig. 9. Iterative procedure in each time step

7. Numerical examples

The aim of the numerical examples is to show the influence of discretization on the accuracy of solutions. The numerical results are compared with the analytical solutions or the results computed by the commercial finite element code. The material of the plates is elastoplastic with linear isotropic hardening obeying the Von Mises yield criterion. The yield stress of the material is σ_Y, Young modulus is E and the tangent modulus is E_t (Fig. 10a). The plates are in the plane stress and are subjected to dynamic impact loading with the Heaviside time dependence. The magnitude of loading is p_o (Fig. 10b). The dimensions of the plates are given in millimetres. The time step of the analysis is the time of propagation of elastic wave along the distance equal to half of the length of the cell.

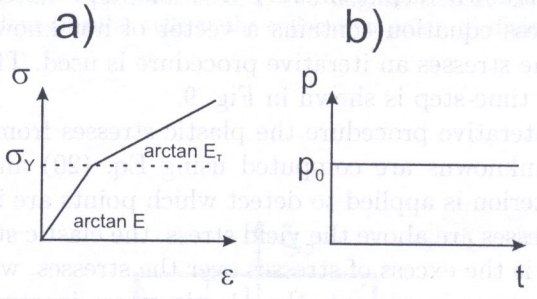

Fig. 10. a) stress–strain relation b) time history of loading

7.1. Rectangular plate – inertial loading

A rectangular plate, shown in Fig. 11a, constrained at two opposite edges moves and is subjected to inertial loads. The acceleration field is uniform within the body. The direction of acceleration is horizontal and its magnitude is $a = 5 \cdot 10^6$ m/s^2. The elastoplastic material of the plate has the following properties: Young modulus $E = 210000$ MPa, tangent modulus $E_t = 5000$ MPa, yield stress $\sigma_Y = 300$ MPa, Poisson ratio $\nu = 0$ and density $\rho = 5000$ kg/m^3. The boundary of the body is divided into 12 quadratic boundary elements and the domain is discretized into 32 constant

interior cells, as shown in Fig. 11b. The numerical results are compared with the analytical solutions. The percentage stress error in each interior cell is given in Fig. 11c. The stress error in each cell is less than 1.3%. The displacements of the upper edge in the horizontal direction, for the elastic and elastoplastic material are shown in Fig. 12. The numerically computed displacements are in very good agreement with the analytical solutions. The maximum displacement for the elastoplastic material is three times bigger than for the elastic material.

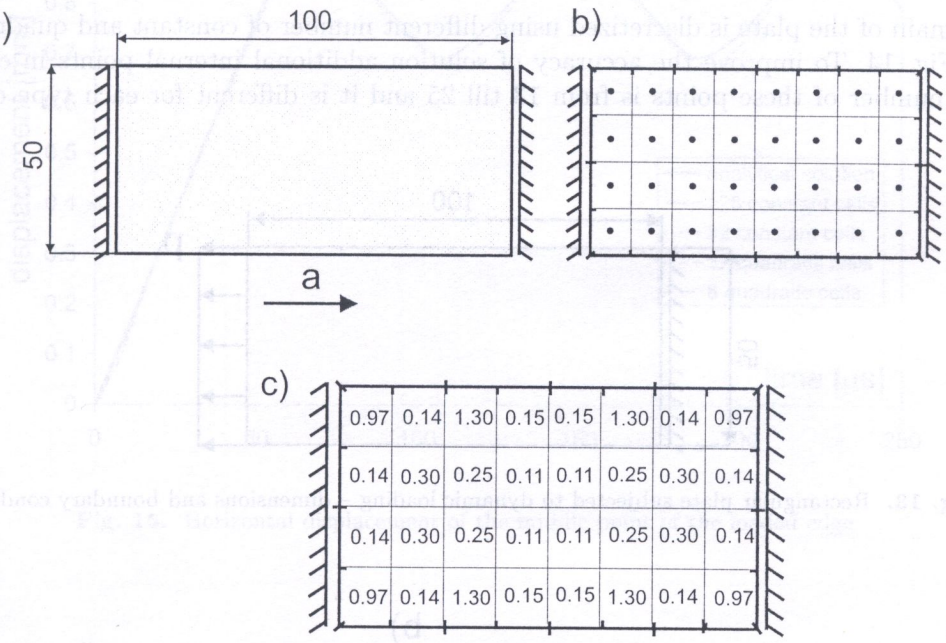

Fig. 11. Rectangular plate subjected to the inertial loading; a) dimensions and boundary conditions, b) discretization, c) percentage stress error in each cell

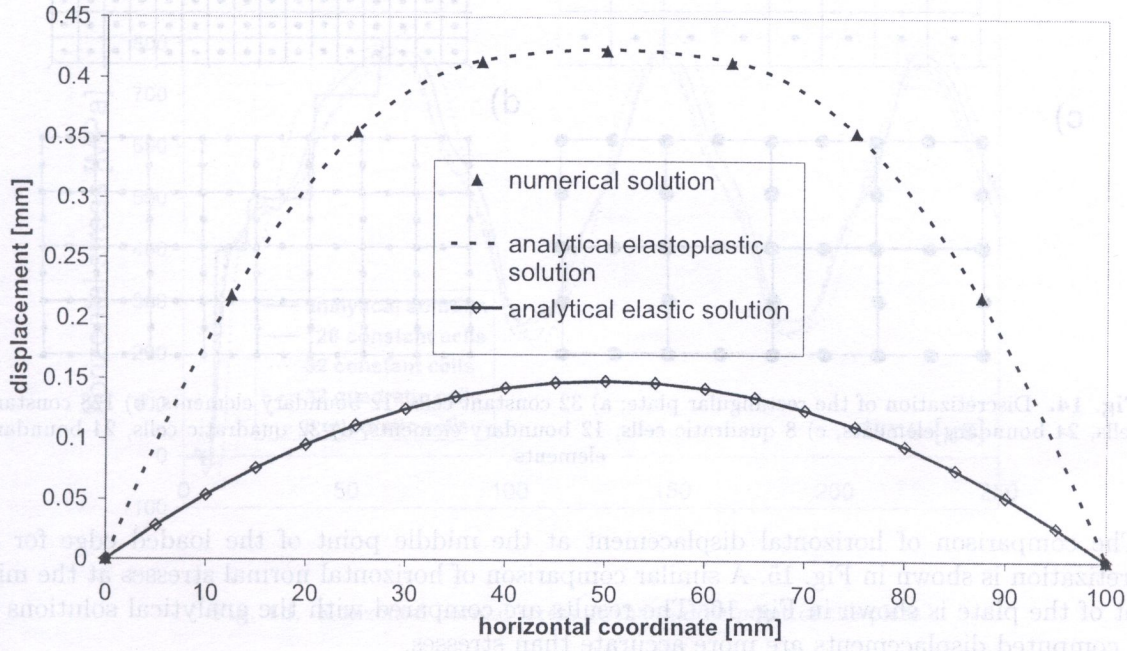

Fig. 12. Displacements of the upper edge of the plate

7.2. Rectangular plate – dynamic loading

A rectangular plate is constrained at one edge and loaded on the opposite edge, as shown in Fig. 13. The material of the plate has the following properties: Young modulus $E = 200000$ MPa, tangent modulus $E_t = 50000$ MPa, yield stress $\sigma_Y = 400$ MPa, Poisson ratio $\nu = 0$ and density $\rho = 8000$ kg/m^3. The plate is subjected to the uniformly distributed impact loading of value $p_0 = 500$ N/mm.

The domain of the plate is discretized using different number of constant and quadratic cells, as shown in Fig. 14. To improve the accuracy of solution additional internal points in each case are used. The number of these points is from 13 till 25 and it is different for each type of discretization.

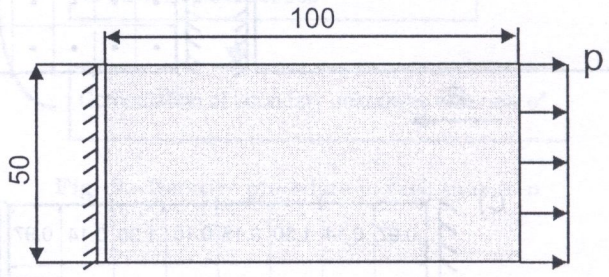

Fig. 13. Rectangular plate subjected to dynamic loading – dimensions and boundary conditions

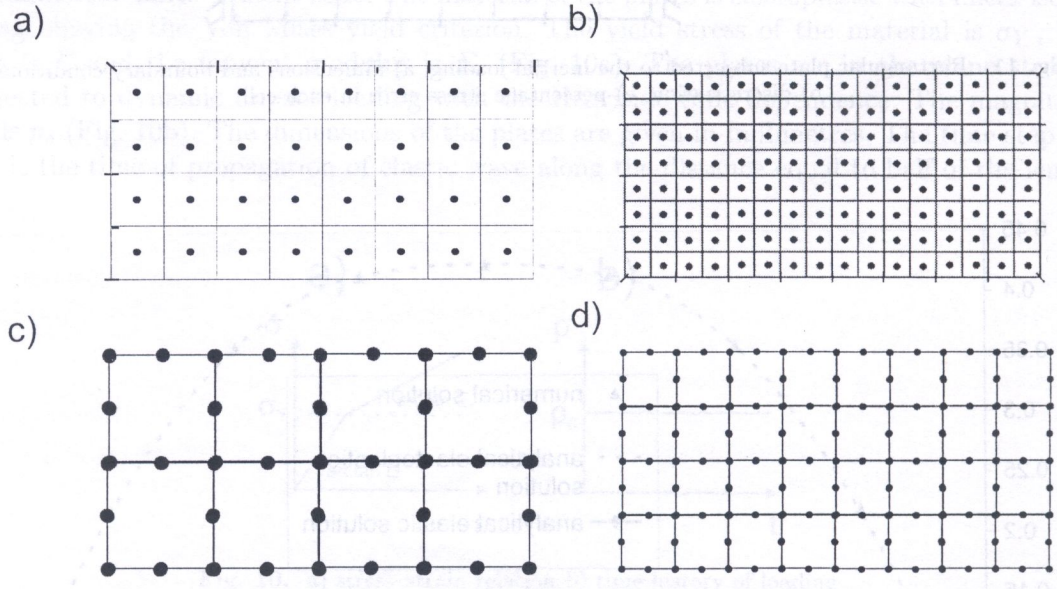

Fig. 14. Discretization of the rectangular plate; a) 32 constant cells, 12 boundary elements, b) 128 constant cells, 24 boundary elements, c) 8 quadratic cells, 12 boundary elements, d) 32 quadratic cells, 24 boundary elements

The comparison of horizontal displacement at the middle point of the loaded edge for each discretization is shown in Fig. 15. A similar comparison of horizontal normal stresses at the middle point of the plate is shown in Fig. 16. The results are compared with the analytical solutions [13]. The computed displacements are more accurate than stresses.

The results show that there are no significant differences between solutions obtained with use of constant and quadratic cells even for the small number of boundary elements and cells.

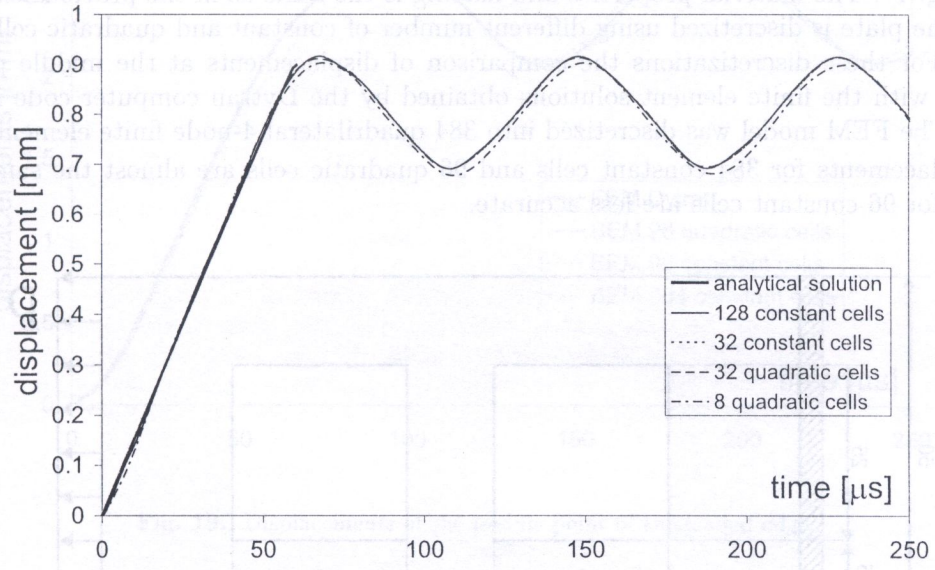

Fig. 15. Horizontal displacement of the middle point of the loaded edge

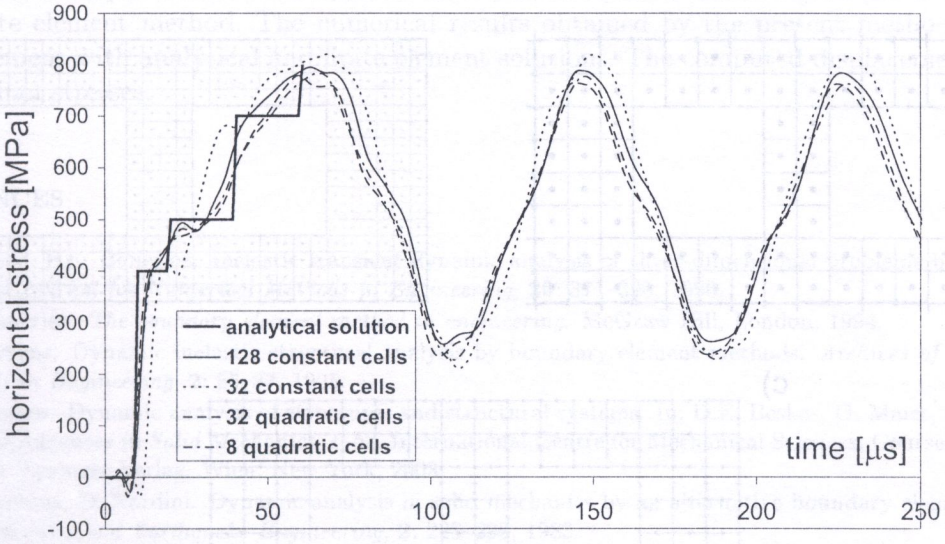

Fig. 16. Horizontal normal stress at the middle point of the plate

7.3. Plate with square holes – dynamic loading

A rectangular plate with quadratic holes constrained at one edge and loaded on the opposite edge is shown in Fig. 17. The material properties and loading is the same as in the previous example. The domain of the plate is discretized using different number of constant and quadratic cells, as shown in Fig. 18. For these discretizations the comparison of displacements at the middle point of the loaded edge with the finite element solutions obtained by the Dytran computer code is presented in Fig. 19. The FEM model was discretized into 384 quadrilateral 4-node finite elements.

The displacements for 384 constant cells and 96 quadratic cells are almost the same. The displacements for 96 constant cells are less accurate.

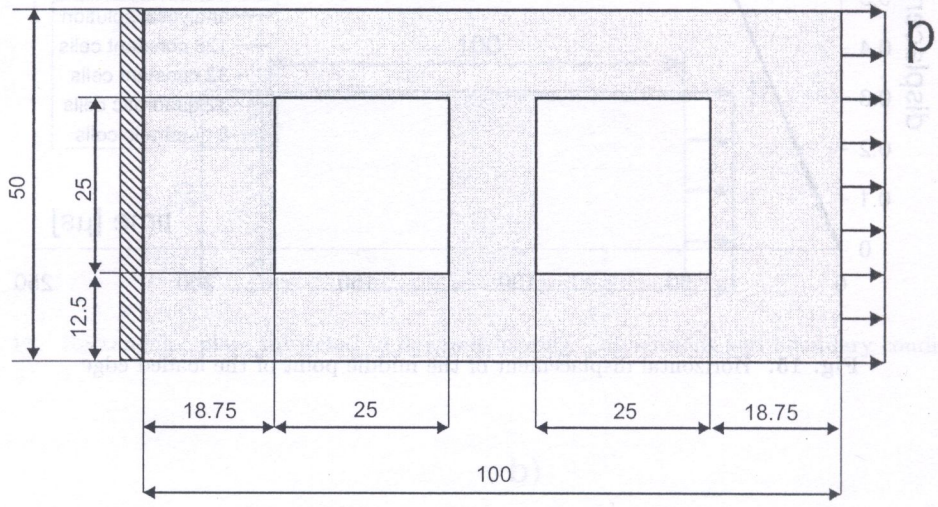

Fig. 17. Plate with square holes subjected to dynamic loading – dimensions and boundary conditions

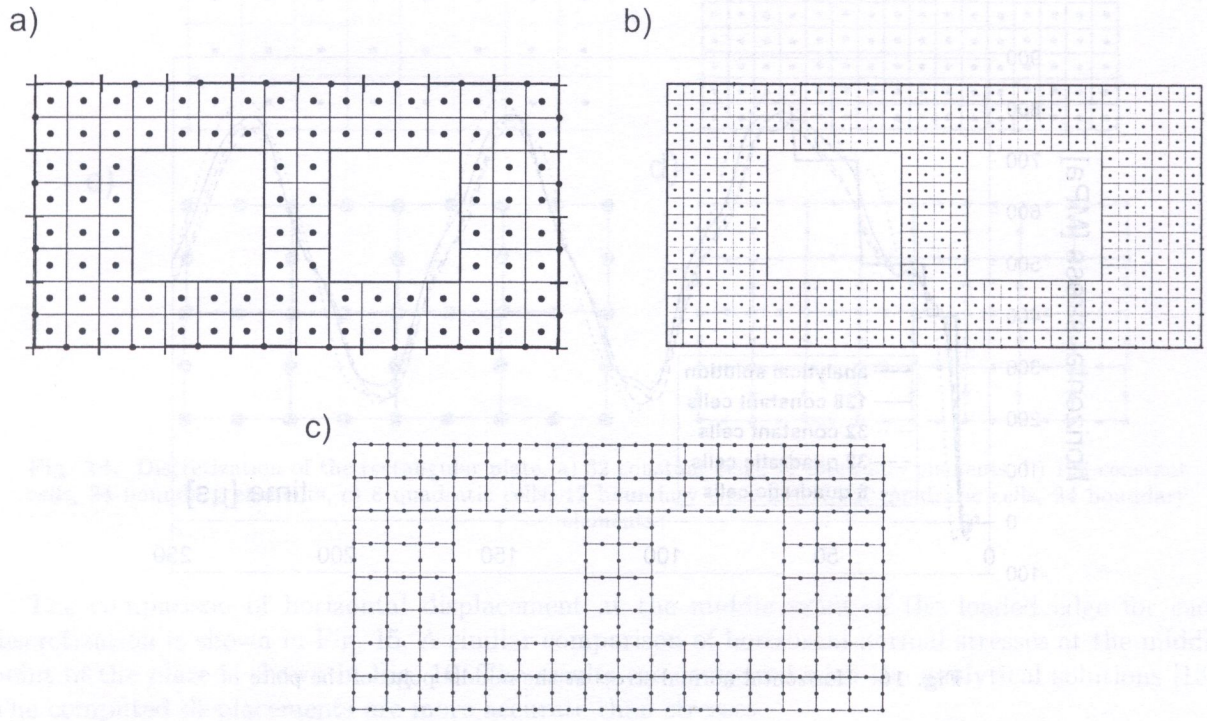

Fig. 18. Discretization of the plate with square holes; a) 96 constant cells, 40 boundary elements, b) 384 constant cells, 80 boundary elements, c) 96 quadratic cells, 40 boundary elements

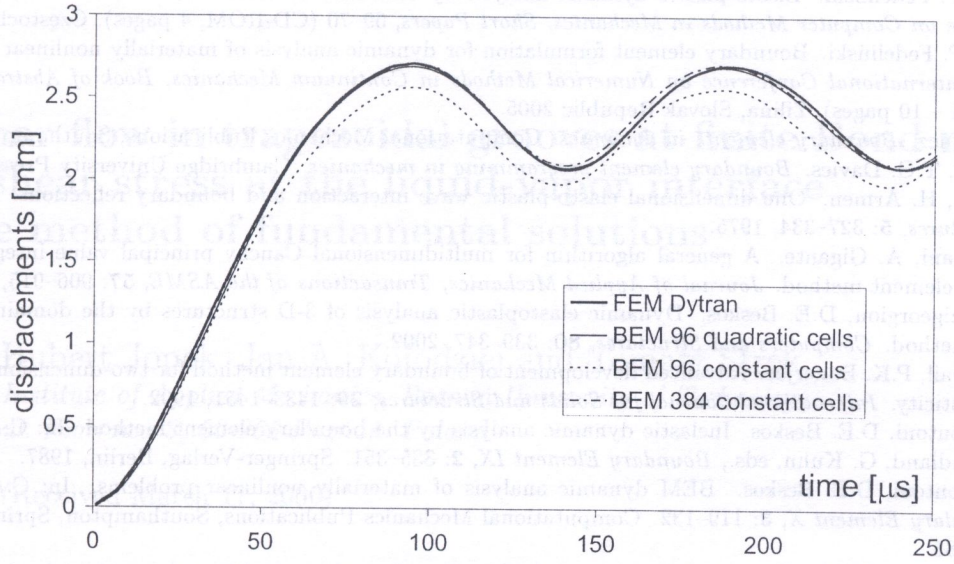

Fig. 19. Displacements of the middle point of the loaded edge

8. Conclusions

In this paper the dual reciprocity boundary element method (DR-BEM) and initial stress approach for elastoplastic plates in plane stress subjected to inertial or dynamic forces is presented. The formulation requires that only the plastic region needs to be discretized. Although the internal cells are introduced they do not increase the number of unknowns in the sets of equations. The paper shows the influence of the domain discretization on the solutions.

The dual reciprocity boundary element method for elastoplastic dynamic analysis gives accurate results and is computationally efficient, because the number of unknowns is much smaller than in the finite element method. The numerical results obtained by the present method are in very good agreement with analytical and finite element solutions. The computed displacements are more accurate than stresses.

References

[1] S. Ahmad, P.K. Banerjee. Inelastic transient dynamic analysis of three-dimensional problems by BEM. *International Journal for Numerical Methods in Engineering*, **29**: 371–390, 1990.

[2] P.K. Banerjee. *The boundary element method in engineering.* McGraw Hill, London, 1994.

[3] D.E. Beskos. Dynamic inelastic structural analysis by boundary element methods. *Archives of Computational Methods in Engineering*, **2**: 55–87, 1995.

[4] D.E. Beskos. Dynamic analysis of structures and structural systems. In: D.E. Beskos, G. Maier, eds., *Boundary Element Advances in Solid Mechanics*, 1–53. International Centre for Mechanical Sciences, Courses and Lectures, No. 440. Springer-Verlag, Wien, New York, 2003.

[5] C.A. Brebbia, D. Nardini. Dynamic analysis in solid mechanics by an alternative boundary element procedure. *Soil Dynamics and Earthquake Engineering*, **2**: 228–233, 1983.

[6] J.A.M. Carrer, J.C.F. Telles. A boundary element formulation to solve transient dynamic elastoplastic problems. *Computers and Structures*, **45**: 707–713, 1992.

[7] H.B. Coda, W.S. Venturini. Dynamic non-linear stress analysis by the mass matrix BEM. *Engineering Analysis with Boundary Elements*, **24**: 623–632, 2000.

[8] T. Czyż, P. Fedeliński. Numerical aspects of modeling elasto-plastic materials by the boundary element method. In: *XLIII Symposium Modeling in Mechanics, Scientific Papers of Department of Applied Mechanics*, **23**: 99–104, Gliwice, 2004.

[9] T. Czyż, P. Fedeliński. Elasto-plastic dynamic analysis by boundary element method. In: *16th International Conference on Computer Methods in Mechanics, Short Papers*, 69–70 (CD-ROM, 4 pages). Częstochowa, 2005.

[10] T. Czyż, P. Fedeliński. Boundary element formulation for dynamic analysis of materially nonlinear structures. In: *10th International Conference on Numerical Methods in Continuum Mechanics, Book of Abstracts*, 21–22, (CD-ROM – 10 pages). Žilina, Slovak Republic 2005.

[11] J. Dominguez. *Boundary elements in dynamics.* Computational Mechanics Publications, Southampton, 1993.

[12] X.W. Gao, T.G. Davies. *Boundary element programming in mechanics.* Cambridge University Press, 2002.

[13] H. Garnet, H. Armen. One dimensional elasto-plastic wave interaction and boundary reflections. *Computers and Structures*, **5**: 327–334, 1975.

[14] M. Guiggiani, A. Gigante. A general algorithm for multidimensional Cauchy principal value integrals in the boundary element method. *Journal of Applied Mechanics, Transactions of the ASME*, **57**: 906–915, 1990.

[15] G.D. Hatzigeorgiou, D.E. Beskos. Dynamic elastoplastic analysis of 3-D structures by the domain/boundary element method. *Computers and Structures*, **80**: 339–347, 2002.

[16] A.S.M. Israil, P.K. Banerjee. Advanced development of boundary element method for two-dimensional dynamic elasto-plasticity. *International Journal for Solids and Structures*, **29**: 1433–1451, 1992.

[17] D.P.N. Kontoni, D.E. Beskos. Inelastic dynamic analysis by the boundary element method. In: C.A. Brebbia, W.L. Wendland, G. Kuhn, eds., *Boundary Element IX*, **2**: 335–351. Springer-Verlag, Berlin, 1987.

[18] D.P.N. Kontoni, D.E. Beskos. BEM dynamic analysis of materially nonlinear problems. In: C.A. Brebbia, ed., *Boundary Element X*, **3**: 119–132. Computational Mechanics Publications, Southampton, Springer-Verlag, Berlin, 1988.

[19] D.P.N. Kontoni, D.E. Beskos. The dual reciprocity boundary element method for the transient dynamic analysis of elastoplastic problems. In: C.A. Brebbia., M.S. Ingber, eds., *Boundary Element Technology VII*, 653–669. Computational Mechanics Publications, Southampton, Elsevier Applied Science, London, 1992.

[20] D.P.N. Kontoni, D.E. Beskos. Transient dynamic elastoplastic analysis by the dual reciprocity BEM. *Engineeering Analysis with Boundary Elements*, **12**: 1–16, 1993.

[21] D.P.N. Kontoni. Elastoplastic dynamic analysis by the DR-BEM in modal co-ordinates. In: H. Pina, C.A. Brebbia, eds., *Boundary Element Technology VIII*, 191–202. Computational Mechanics Publications, Southampton, Boston, 1993.

[22] D. Nardini, C.A. Brebbia. A new approach to free vibration analysis using boundary elements. *Applied Mathematical Modelling*, **7**: 157–162, 1983.

[23] J.C.F. Telles. The boundary element method applied to inelastic problems. In: C.A. Brebbia, S.A. Orszag, eds., *Lecture Notes in Engineering.* Springer-Verlag, Berlin, 1983.

[24] J.C.F. Telles, J.A.M. Carrer. Implicit solution techniques for inelastic boundary element analysis. In: C.A. Brebbia, ed., *Boundary Element X*, **3**: 3–15. Computational Mechanics Publications, Southampton, Springer-Verlag, Berlin, 1988.

[25] J.C.F. Telles, J.A.M. Carrer. Static and transient dynamic nonlinear stress analysis by the boundary element method with implicit techniques. *Engineering Analysis with Boundary Elements*, **14**: 65–74, 1994.

[26] J.C.F. Telles, J.A.M. Carrer, W.J. Mansur. Transient dynamic elastoplastic analysis by the time-domain BEM formulation. *Engineering Analysis with Boundary Elements*, **23**: 479–486, 1999.